Can edge AI mitigate environmental effects on camera trap performance?

Taylor L. Kaltenback, Jeffrey C. Mosley, Lance B. McNew, Jared T. Beaver

Kaltenbach, T. L., Mosley, J. C., McNew, L. B., & Beaver, J. T. (2025). Can edge AI mitigate environmental effects on camera trap performance?. Wildlife Society Bulletin, 49(3), e1598.

DOI: 10.1002/wsb.1598

Received: 18 September 2024 | Revised: 10 March 2025 | Accepted: 14 March 2025

DOI: 10.1002/wsb.1598

RESEARCH ARTICLE

Can edge AI mitigate environmental effects on camera trap performance?

Taylor L. Kaltenbach | Jeffrey C. Mosley | Lance B. McNew | Jared T. Beaver

Department of Animal and Range Sciences, Montana State University, Bozeman, Montana 59717, USA

Correspondence
Taylor L. Kaltenbach, P.O. Box 172900, Bozeman, Montana, USA.
Email: taylorkaltenbach@montana.edu

Funding information
Montana State University, Grant/Award Number: 432047

Abstract

Abiotic and biotic conditions can affect camera trap performance, and failure to account for environmental factors can bias wildlife research and management inferences modeled from camera trap data. We investigated whether a camera trap enabled with edge artificial intelligence (AI) could mitigate environmental effects on camera trap performance. We compared an edge AI-enabled prototype with 2 camera trap models commonly used by wildlife managers and researchers in a field experiment in the Greater Yellowstone Ecosystem of south-central Montana, USA. Camera trap performance was affected by air temperature, wind speed, and time of day. Increased air temperatures and wind speeds decreased the conditional probability of positive detections, and the edge AI-enabled prototype did not mitigate these effects. The conditional probability of positive detections was <0.15 when air temperatures were ≥30°C or wind speeds were ≥15 km/h. However, when air temperatures were ≥30°C, the conditional probability of false positives was nearly zero for the edge AI-enabled prototype vs. 0.10 to 1.00 for the camera traps without AI, thereby making image collection and analysis more efficient. Air temperature had no effect on missed detections during crepuscular periods, but during daytime, the conditional probability of missed detections was >0.15 when air temperatures were ≥30°C. During nighttime, the conditional

probability of missed detections decreased as air temperature increased, with the conditional probability of missed detections <0.25 when air temperatures were ≥30°C. The edge AI-enabled prototype did not mitigate time-of-day effects on the conditional probability of missed detections, and the edge AI-enabled prototype was more likely to miss detections than camera traps without AI. The conditional probability of missed detections ranged from 0.20 to 0.80 for the edge AI-enabled prototype vs. 0.05 to 0.50 for the camera traps without AI. As AI technology advances, edge AI-enabled camera traps must limit missed detections while continuing to minimize false positives during warm conditions.

KEYWORDS

camera trap, detection probability, edge artificial intelligence, environmental conditions, Greater Yellowstone Ecosystem, Montana, passive monitoring, remote sensing

Camera trapping is a non-invasive, safe, and labor-saving method for surveying wildlife (Cutler and Swann 1999, Burton et al. 2015, Swanson et al. 2015). However, abiotic and biotic conditions affect whether a camera trap captures positive detections (i.e., when a camera trap triggers and an animal is present) or false positive images (i.e., when a camera trap triggers but no animal is present; Swann et al. 2004, Newey et al. 2015). Failure to account for environmental factors can bias research and management inferences modeled from camera trap data (Burton et al. 2015, Hofmeester et al. 2019).

Modern camera traps use passive infrared (PIR) sensors that monitor infrared radiation (i.e., thermal energy) emitted from the surface of objects within a camera trap's detection zone. A camera trap triggers when the PIR sensor detects an increase or decrease in thermal energy relative to the background object surfaces (Meek et al. 2012, Welbourne et al. 2016). Air temperatures affect camera trap detections by altering the surface temperatures of both background objects and wildlife (Swann et al. 2004, Welbourne et al. 2016, Jacobs and Ausband 2018). Rain, snow, and fog can reduce camera trap detection distances (Kays et al. 2009, Rowcliffe et al. 2011), and vegetation moving in the wind can intermittently shade background objects from the sun, causing surface temperatures to fluctuate and hinder camera trap performance (Gregory et al. 2014, Jacobs and Ausband 2018). Wind speed, humidity, cloud cover, and time-of-day effects on camera trap performance have been evaluated less extensively, but they are known to affect infrared thermography, which employs thermal sensors similar to those used in most camera traps. Greater humidity and wind speed reduce the ability of thermal imaging to detect wildlife because water vapor in the air absorbs infrared radiation emitted by wildlife and wind cools the surface of animal bodies thereby reducing the infrared radiation they emit (Cilulko et al. 2013, Havens and Sharp 2015). Conversely, thermal imaging is better able to detect wildlife when cloud cover moderates solar insolation that would otherwise be absorbed and re-emitted by background surfaces, and during pre-dawn hours the background surface temperatures are lowest, accentuating the thermal contrasts with wildlife (Bernatas and Nelson 2004, Havens and Sharp 2015).

In addition to affecting positive detections, environmental conditions also influence the capture of false positive images by camera traps. False positive images are captured when non-animal thermal heterogeneity within the detection zone causes the camera trap to trigger when no animal is present. False positive triggers may also be influenced by functional differences among camera trap models, such as the sensitivity of PIR sensors (i.e., the threshold of thermal difference that results in the camera trap triggering), the size of camera trap detection zones, and trigger

speeds (i.e., the time interval between a PIR sensor detecting a thermal anomaly and the camera triggering; Swann et al. 2004, Wellington et al. 2014, Rovero and Zimmermann 2016). Captures of false positive images are problematic because they occupy storage on the camera trap's SD card, drain battery power, and increase the time required to process images (Newey et al. 2015, Heiniger and Gillespie 2018). False positives can contribute to missed detections if an animal enters and exits a camera trap's detection zone during the camera's delay time after triggering to capture a false positive. Practical strategies for limiting false positives include orienting camera traps to face north or northeast in the northern hemisphere (Hughson et al. 2010) or south or southeast in the southern hemisphere, clearing vegetation from near the camera trap's lens (Gregory et al. 2014, Zimmermann and Rovero 2016, Apps and Hutt 2018), and setting the camera trap's delay time between triggers to be as brief as possible. However, additional methods to further reduce or eliminate false positive triggers would enhance the efficiency of camera trap surveys. A global survey of camera trap users among researchers and conservationists determined that resistance to environmental conditions and automated filtering of false positives were among the most needed technological developments (Glover-Kapfer et al. 2019).

Incorporating edge artificial intelligence (AI) technology could be one way to enhance the performance of camera traps. The term edge AI reflects that a device uses AI algorithms to analyze data locally rather than offloading the data for analysis by external systems (e.g., cloud infrastructure). Recently, Whytock et al. (2023) and Dertien et al. (2023) implemented edge AI in camera trap systems in central Africa and India, respectively, to analyze wildlife images post-capture. In our study, we investigated an edge AI-enabled camera trap that analyzed thermal anomalies before triggering to capture images, which we theorized would improve camera trap performance. Specifically, we assessed whether edge AI applied before image capture could mitigate the influence of environmental conditions on camera trap performance. We hypothesized that our edge AI-enabled prototype would be less affected by environmental conditions than contemporary camera traps without AI.

STUDY AREA

We conducted our field experiment at mid-elevation sites (circa 2,000 m) southwest of Emigrant, MT, USA, about 8 km north of Yellowstone National Park (YNP) within the Northern Yellowstone Range (NYR) and the Greater Yellowstone Ecosystem (Mosley et al. 2018). Outside of YNP, the NYR is a working landscape comprised of multiple-use federal and state lands, ranches, and other private lands that provide critical habitat for wildlife (Mosley et al. 2018). Eight species of wild ungulates inhabit the NYR: bison (*Bison bison*), Rocky Mountain elk (*Cervus elaphus nelsoni*), Rocky Mountain mule deer (*Odocoileus hemionus hemionus*), white-tailed deer (*O. virginianus canadensis*), moose (*Alces alces*), pronghorn (*Antilocapra americana*), Rocky Mountain bighorn sheep (*Ovis canadensis canadensis*), and mountain goats (*Oreamnos americanus*). Domestic ungulates cohabit portions of the NYR, including cattle, sheep, and horses, as do several ungulate predators: grizzly bears (*Ursus arctos horribilis*), black bears (*Ursus americanus*), coyotes (*Canis latrans*), mountain lions (*Puma concolor*), and northern Rocky Mountain gray wolves (*C. lupus*; Mosley and Mundinger 2018). Vegetation generally consists of irrigated pastures and hayfields at low elevations, foothill grasslands and sagebrush steppe at mid-elevations, and conifer forests at mid- to higher elevations. Dominant native plant species include bluebunch wheatgrass (*Pseudoroegneria spicata*), Idaho fescue (*Festuca idahoensis*), Columbia needlegrass (*Stipa nelsoni*), mountain big sagebrush (*Artemisia tridentata* ssp. *vaseyana*), lodgepole pine (*Pinus contorta*), and Douglas-fir (*Pseudotsuga menziesii*; Pfister et al. 1977, Mueggler and Stewart 1980).

METHODS

We evaluated whether an edge AI-enabled camera trap prototype (Grizzly Systems Inc., Emigrant, MT, USA) could effectively mitigate environmental effects on camera trap performance. We compared the edge AI-enabled prototype with 2 commercially available camera traps without AI: the Browning Strike Force APEX (Prometheus Group

LLC, Birmingham, AL, USA) and the Reconyx Hyperfire 2 (Reconyx, Inc., Holmen, WI, USA). Both are commonly used by wildlife managers and researchers (Monterroso et al. 2020, Jessop et al. 2021, Palencia et al. 2023). The edge AI-enabled camera trap prototype featured a quad-element PIR sensor with an ultra-low power AI trigger that analyzed thermal anomalies detected by the PIR sensor before triggering to capture an image. A machine learning algorithm ran a binary classifier on the thermal radiation data captured by the PIR sensor, making an alive or not alive determination that either triggered or did not trigger the camera to capture an image.

We compared the performance of the 3 camera trap models using methods similar to those described by Jacobs and Ausband (2018). One camera trap of each model (Browning, Reconyx, and edge AI-enabled prototype) comprised a camera trap group. We mounted the camera traps side by side, 10 cm apart, on a wooden board. We randomized the position of the camera trap models so that no camera trap model was consistently on the left, middle, or right positions on the boards. We attached the boards to trees, wooden fence posts, or steel t-posts approximately 75 cm above ground level to optimize the detection of large mammals, specifically Rocky Mountain elk, grizzly bears, and northern Rocky Mountain gray wolves. We aimed the camera traps parallel to the ground surface, programmed the camera traps to capture images 24 hr/day, and oriented the camera traps northward to avoid capturing sun-blurred images.

We deployed 10 camera trap groups from 15 June–15 September 2023. We placed the camera trap groups using feature-based site placement to maximize exposure to wildlife (e.g., creek crossings and game trails; Iannarilli et al. 2021). All 10 camera trap groups were deployed on private land, spaced at least 100 m apart, and placed so their fields of view did not overlap. We set all camera traps to high sensitivity and to capture one image per trigger. We set the delay times between trigger events to be as similar as possible among the 3 camera trap models, with the Browning and Reconyx camera traps set to 5-second delays and the edge AI prototype to a 3-second delay. We enclosed each camera trap group within a 1.2-m high woven wire fence to prevent damage from wildlife or livestock. To reduce false positives resulting from uneven heating of vegetation, we cleared all vegetation within 1 m of each camera trap's lens during the camera traps' initial deployments (Gregory et al. 2014, Zimmermann and Rovero 2016, Apps and Hutt 2018). Similarly, we removed vegetation during our weekly visits to the camera sites to exchange SD cards and monitor battery power levels. We did not remove vegetation farther from the cameras to avoid affecting wildlife behavior (Apps and Hutt 2018).

Environmental variables

We monitored 6 environmental variables to evaluate their effects on camera trap performance: air temperature (°C), relative humidity (%), wind speed (km/h), cloud cover (%), vegetation type (forest, grassland), and time of day (daytime, nighttime, crepuscular). We selected these environmental variables based on their ease of measurement and interpretability, relevance to the effect on thermal reflectance within a camera trap's detection zone, and their significance as established by previous studies on the performance of camera traps or similar thermal sensors (Swann et al. 2004, Havens and Sharp 2015, Jacobs and Ausband 2018). We remotely monitored weather variables at each camera trap site using a Kestrel 5500 weather meter (Nielsen-Kellerman, Boothwyn, PA, USA) programmed to record measurements every 10 minutes. We downloaded weather data from the camera trap sites at 2-week intervals. We collected satellite cloud cover data from the GOES-16 Advanced Baseline Imager Level 2 Clear Sky Mask product, which categorized cloud cover as present or absent at 5-minute intervals and 2-km resolution (Heidinger and Straka 2012, Heidinger et al. 2020). We classified the vegetation type at each camera trap site as either grassland ($n = 5$ sites) or forest ($n = 5$ sites) based on the predominant vegetation within the camera traps' fields of view. We assigned 1 of 3 time periods (daytime, nighttime, or crepuscular) to each camera trap image. We defined daytime as 1 hour after sunrise to 1 hour before sunset; we defined nighttime as 1 hour after sunset to 1 hour before sunrise; and we defined crepuscular as the 2-hour period surrounding sunrise and sunset (Rockhill et al. 2013, Mosley et al. 2020).

Image processing

We deleted all images of humans and vehicles before data analysis. We also removed from the dataset any images captured within 5 minutes before or after camera trap checks and any images captured when 1 or more camera traps in a group were non-functioning. We excluded all data from 1 forest site and 1 grassland site due to equipment malfunctions.

We used ExifTool software to modify image metadata to reflect the start time of the camera trap group (Exiftool version 12.41, exiftool.org, accessed 17 Jul 2022), which standardized the timestamp associated with each image and accounted for instances when we incorrectly set the date and time in the field. We then renamed the images from each camera trap using a modified version of the Image Renamer R script (Wildlife Coexistence Lab, github.com/WildCoLab, accessed 17 Jul 2023), which provided each image with a unique label containing the camera trap ID and the image timestamp. We used Timelapse2 software (Greenberg et al. 2019) to manually annotate all images and record blank images and positive detections.

The 3 camera trap models captured images at different rates. Therefore, we could not compare individual images among the camera trap models in each group. Instead, we aggregated each group's images into 2-minute event bins (i.e., 2-minute segments when at least 1 camera in the group triggered). For each camera trap model × event bin combination, we classified camera trap performance to be either a positive detection, false positive, or missed detection. We classified camera trap model × event bin combinations as positive detections when they included an image with an animal present. Conversely, if a camera trap model × event bin combination included only blank images (i.e., no animal in an image) and no other camera trap model in its group had captured a positive detection during the same event bin, then we classified the camera trap model × event bin combination as a false positive. Finally, if a camera trap model × event bin combination included only blank images (i.e., no animal in any image) or no images at all, but at least 1 of the other camera trap models in its group captured a positive detection during the same event bin, then we classified the camera trap model × event bin combination as a missed detection.

Data analysis

We used generalized linear mixed models with a binomial error distribution and logit-link function (Hosmer and Lemeshow 2000) to contrast positive detections (yes/no), false positives (yes/no), and missed detections (yes/no). Given that we did not know the true probability that an animal was or was not present at camera sites during the 2-minute event bins, we evaluated the conditional probabilities of positive detections, missed detections, and false positives. The conditional event was that at least 1 camera in its group triggered during the 2-minute event bin. These conditional probabilities reflect the behaviors of the animal populations and environmental conditions in the Northern Yellowstone Range from mid-June to mid-September 2023. Other animal populations and environmental conditions might influence the conditional probabilities of detection differently.

Before developing our candidate models, we evaluated our weather variables for multicollinearity by calculating pairwise Spearman's rank correlations. If we detected a correlation between a pair of predictor variables ($|r| > 0.70$; Green 1979), we retained the variable that contributed most to the interpretation of camera trap performance and eliminated the other variable from analyses (Hosmer and Lemeshow 2000). A strong correlation was detected between relative humidity and air temperature ($|r| = 0.86$); therefore, we excluded relative humidity from the analysis. The correlation between all other variables was <0.70.

We developed 37 candidate models based on our *a priori* hypotheses about the effects of environmental conditions on camera trap performance (Table 1; Burnham and Anderson 2002). The edge AI-enabled camera trap prototype served as the reference category, and we included individual camera trap IDs as a random effect to account for repeated observations from camera traps and to limit Type I errors. We standardized environmental

TABLE 1 Candidate models for evaluating the effects of environmental conditions on camera trap performance during summer 2023 in south-central Montana, USA.

Model	Description
Null	Null model
Model 1	Camera trap model
Model 2	Temperature
Model 3	Wind speed
Model 4	Cloud cover
Model 5	Vegetation type
Model 6	Time of Day
Model 7	Temperature + wind speed + temperature × wind speed
Model 8	Temperature + cloud cover + temperature × cloud cover
Model 9	Temperature + vegetation type + temperature × vegetation type
Model 10	Temperature + time of day + temperature × time of day
Model 11	Wind speed + cloud cover + wind speed × cloud cover
Model 12	Wind speed + vegetation type + wind speed × vegetation type
Model 13	Wind speed + time of day + wind speed × time of day
Model 14	Cloud cover + vegetation type + cloud cover × vegetation type
Model 15	Cloud cover + time of day + cloud cover × time of day
Model 16	Vegetation type + time of day + vegetation type × time of day
Model 17	Camera trap model + temperature
Model 18	Camera trap model + wind speed
Model 19	Camera trap model + cloud cover
Model 20	Camera trap model + vegetation type
Model 21	Camera trap model + time of day
Model 22	Camera trap model + temperature + wind speed + cloud cover + vegetation type + time of day
Model 23	Camera trap model + temperature + camera trap model × temperature
Model 24	Camera trap model + wind speed + camera trap model × wind speed
Model 25	Camera trap model + cloud cover + camera trap model × cloud cover
Model 26	Camera trap model + vegetation type + camera trap model × vegetation type
Model 27	Camera trap model + time of day + camera trap model × time of day
Model 28	Camera trap model + temperature + wind speed + temperature × wind speed
Model 29	Camera trap model + temperature + cloud cover + temperature × cloud cover
Model 30	Camera trap model + temperature + vegetation type + temperature × vegetation type
Model 31	Camera trap model + temperature + time of day + temperature × time of day
Model 32	Camera trap model + wind speed + cloud cover + wind speed × cloud cover
Model 33	Camera trap model + wind speed + vegetation type + wind speed × vegetation type

TABLE 1 (Continued)

Model	Description
Model 34	Camera trap model + wind speed + time of day + wind speed × time of day
Model 35	Camera trap model + cloud cover + vegetation type + cloud cover × vegetation type
Model 36	Camera trap model + cloud cover + time of day + cloud cover × time of day
Model 37	Camera trap model + vegetation type + time of day + vegetation type × time of day

variables before modeling to improve model convergence (Schielzeth 2010), but we present our results using unstandardized values.

We assessed the strength of evidence for each candidate model with Akaike's Information Criterion adjusted for small sample size (AIC_c), and we ranked all models by calculating ΔAIC_c (Δ_i: the difference in AIC_c between the lowest-AIC_c model and AIC_c for each candidate model). Per Burnham and Anderson (2002), we considered the model with the lowest AIC_c value to be the model that best explained camera trap performance. We also examined additional models if $\Delta AIC_c \leq 2$ (Burnham and Anderson 2002). For each parameter estimate in the top-ranked model, we calculated 85% CI (Arnold 2010). If the 85% CI of any parameter coefficient overlapped zero, we considered these covariates uninformative (Arnold 2010). We created visualizations for the top-ranked candidate models using the ggeffects package (Lüdecke 2018) and, when applicable, we held non-focal variables at their means. We performed all analyses in R (Program R, version 4.3.1, Foundation for Statistical Computing, Vienna, Austria).

RESULTS

Our analysis included 8,614 event bins, encompassing 49,859 images. Positive detections ($n = 39{,}379$ images) included arthropods, black bears, cattle, coyotes, domestic dogs, elk, grizzly bears, horses, moose, mountain lions, mule deer, pronghorns, red foxes (*Vulpes vulpes*), sandhill cranes (*Grus canadensis*) and other birds, white-tailed deer, and gray wolves. Air temperature and wind speed at the camera trap sites averaged (±SE) 21.6 ± 0.1°C (range: −1 to 40.9°C) and 3.1±0.1 km/h (range: 0 to 25.9 km/h), respectively, during the 3-month study period. Thirty-nine percent of event bins occurred when clouds were above the camera trap sites.

The candidate model containing camera trap model, air temperature, and camera trap model × air temperature interaction received the most support for characterizing the conditional probability of capturing false positives ($\Delta AIC_c = 0$ and $w_i = 1.00$; Table 2). The candidate model containing camera trap model, air temperature, wind speed, and air temperature × wind speed interaction received the most support for characterizing the conditional probability of capturing positive detections ($\Delta AIC_c = 0$ and $w_i = 0.96$; Table 2). The candidate model containing camera trap model, air temperature, time of day, and air temperature × time of day interaction received the most support for characterizing the conditional probability of missed detections ($\Delta AIC_c = 0$ and $w_i = 0.98$; Table 2). Neither cloud cover nor vegetation type had substantive effects on the conditional probabilities of capturing positive detections, false positives, or missed detections (Table 2).

We found support for an interaction between air temperature and camera trap model on the conditional probability of capturing false positives (Table 3). As air temperature increased, the edge AI-enabled prototype was less likely to capture false positives than the Browning or Reconyx camera traps (Figure 1). When air temperatures were ≥30°C, the conditional probability of false positives was nearly zero for the edge AI-enabled prototype vs. 0.10 to 1.00 for the camera traps without AI.

The conditional probability of positive detections decreased as air temperature increased (Table 3; Figure 2). The conditional probability of positive detections was <0.15 when air temperatures were ≥30°C. We did not find

TABLE 2 Fit statistics for the top 3 candidate models and null model evaluating environmental effects on camera trap performance. Models are ranked by Akaike Information Criterion (AIC_c), K is the number of fixed effects, Δ AIC_c is the difference of each model's AIC_c value from that of the highest ranked model, and w_i is the Akaike weight (sum of all Akaike weights = 1.00).

Model	K[a]	AIC_c	Δ AIC_c	w_i	Cumulative w_i
False Positives					
Camera trap model + temperature + camera trap model × temperature	7	12916.61	0	1	1.00
Camera trap model + temperature + vegetation type + temperature × vegetation type	7	13581.64	665.03	0	1.00
Temperature + vegetation type + temperature × vegetation type	5	13597.67	681.06	0	1.00
Null	2	15572.60	2655.99	0	1.00
Positive Detections					
Camera trap model + temperature + wind speed + temperature × wind speed	7	20457.12	0	0.96	0.96
Temperature + wind speed + temperature × wind speed	5	20463.70	6.58	0.04	1.00
Camera trap model + temperature + wind speed + cloud cover + vegetation type + time of day	10	20528.21	71.09	0	1.00
Null	2	24502.10	4044.98	0	1.00
Missed Detections					
Camera trap model + temperature + time of day + temperature × time of day	9	10187.16	0	0.98	0.98
Camera trap model + temperature + camera trap model × temperature	7	10194.77	7.62	0.02	1.00
Camera trap model + temperature + wind speed + cloud cover + vegetation type + time of day	10	10202.35	15.194	0	1.00
Null	2	10263.26	76.11	0	1.00

[a]All models included random intercepts for individual camera traps.

evidence that the air temperature and camera trap model interacted to influence the conditional probability of positive detections or missed detections (Table 3).

For missed detections, we found support for an interaction between air temperature and time of day (Table 3). The air temperature had no effect during crepuscular periods, but during daytime, the conditional probability of missed detections increased with increasing air temperature (Figures 3A and 3B). The conditional probability of missed detections was >0.15 when air temperatures were ≥30°C. During nighttime, the conditional probability of missed detections decreased with warmer temperatures (Figure 3C). The conditional probability of missed detections during nighttime was <0.25 when air temperatures were ≥30°C. The time of day did not influence the conditional probabilities of capturing false positives or positive detections (Table 3).

Wind speed affected the conditional probability of capturing positive detections, but wind speed did not affect the conditional probability of capturing false positives or missed detections (Table 3). The conditional probability of capturing positive detections decreased as wind speed increased. The conditional probability of positive detections was <0.15 when wind speeds were ≥15 km/h. We did not find support for an interaction between wind speed and the camera trap model (Table 3; Figure 4), but there was support for an interaction between wind speed and air

TABLE 3 Model coefficients (β), standard errors (SE), and 85% confidence intervals (CIs) of the top-ranked model for each camera performance variable. "Browning" and "Reconyx" were indicator variables of the nominal variable "camera trap model." The edge AI-enabled camera trap prototype was the reference category.

Camera Performance Variable	β	SE	85% CI (β)	
			Lower	Upper
False Positives				
Edge AI prototype (intercept)	−4.62	0.42	−5.23	−4.01
Browning	4.60	0.63	3.70	5.50
Reconyx	1.86	0.61	0.98	2.74
Temperature	−1.02	0.09	−1.15	−0.89
Browning × temperature	2.66	0.10	2.52	2.80
Reconyx × temperature	1.52	0.10	1.37	1.66
Positive Detections				
Edge AI prototype (intercept)	−2.55	0.30	−2.99	−2.11
Browning	1.62	0.46	0.96	2.29
Reconyx	1.01	0.45	0.36	1.66
Temperature	−1.28	0.03	−1.32	−1.24
Wind speed	−0.46	0.03	−0.50	−0.42
Temperature × wind speed	−0.55	0.04	−0.60	−0.50
Missed Detections				
Edge AI prototype (intercept)	0.43	0.28	0.04	0.75
Browning	−2.22	0.34	−2.72	−1.73
Reconyx	−1.36	0.34	−1.85	−0.87
Temperature	0.04	0.11	−0.09	0.16
Time of Day (day)	0.03	0.16	−0.29	0.00
Time of Day (night)	−0.62	0.33	−0.49	0.06
Temperature × time of day (day)	0.23	0.11	0.05	0.32
Temperature × time of day (night)	−0.56	0.22	−0.70	−0.20

temperature (Table 3). Low air temperatures mediated the negative effect of wind speed on the conditional probability of positive detections (Figure 5). Even at wind speeds ≥25 km/h, the conditional probability of capturing positive detections did not decline until air temperature reached ≥10°C.

DISCUSSION

The PIR sensors in camera traps detect infrared radiation emitted from the surfaces of objects within the camera trap's detection zone. Passive infrared sensors cause camera traps to trigger and capture an image when they detect an object emitting a sufficiently higher or lower amount of infrared radiation than background objects (Welbourne et al. 2016). However, camera traps are not all built the same (Meek and Pittet 2012, Meek et al. 2015), and our

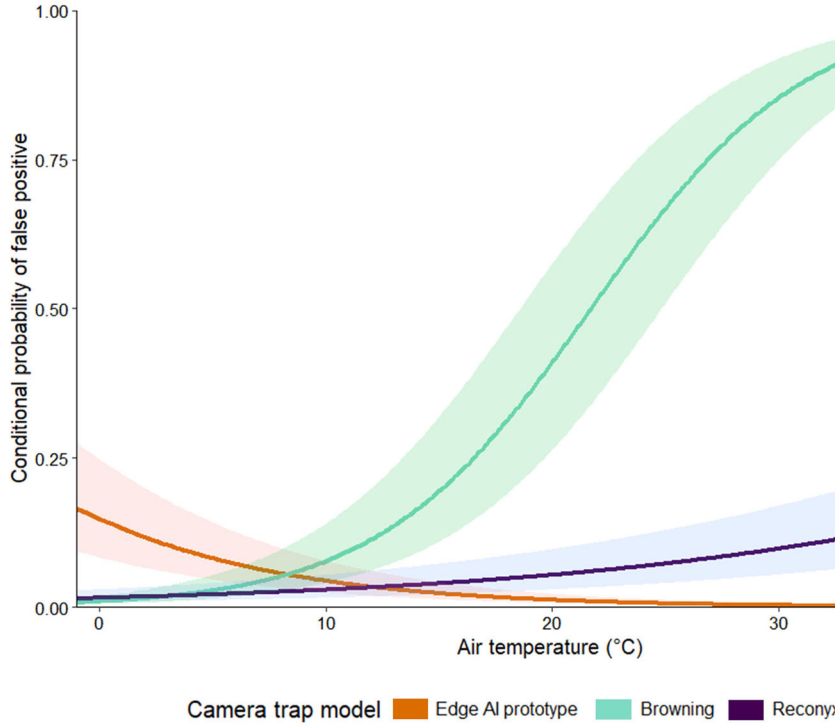

FIGURE 1 Influence of air temperature on the predicted conditional probability of false positives among 3 camera trap models during summer 2023 in south-central Montana, USA. Shaded areas represent 85% confidence intervals.

results support recommendations that differences in PIR sensitivity among camera trap models must be accounted for during data analyses when wildlife surveys incorporate data gathered from more than 1 camera trap model (Damm et al. 2010, Burton et al. 2015, Hofmeester et al. 2019). Our study highlights the complex interplay between air temperature, wind speed, time of day, and camera trap model on detection probabilities, and it offers valuable insights into the potential of edge AI technology to mitigate some of these challenges.

Air temperature affected the performance of all 3 camera trap models. While the edge AI-enabled camera trap prototype in our study did not mitigate the effects of air temperature on positive detections or missed detections, it was less likely to capture false positives when air temperatures were warmer than the camera trap models without AI. At air temperatures ≥15°C, the edge AI-enabled prototype was less likely to capture false positives than Browning, and the edge AI-enabled prototype was less likely to capture false positives than Reconyx at air temperatures ≥20°C. The edge AI-enabled prototype achieved these results despite having a wider detection zone than the Browning or Reconyx camera traps (detection angles of 55° vs. 42.2° and 45.2°, respectively). Previous research documented that camera traps with wider detection zones are more likely to capture false positives (Swann et al. 2004). The time of day interacted with air temperature to affect the conditional probability of missed detections by all 3 camera trap models. At night, the conditional probability of missed detections decreased as air temperature increased. However, the relationship reversed during daytime when the conditional probability of missed detections increased as air temperature increased. We suggest our results reflect differences in thermal biology. Homeothermic animals exposed to high air temperatures dissipate heat by increasing blood flow in the capillaries closest to their skin, which increases the amount of radiation the animals emit (Montanholi et al. 2008, Mota-Rojas et al. 2024). When high air temperatures occur at night, the increased radiation emissions from animals coincide with lower emissions

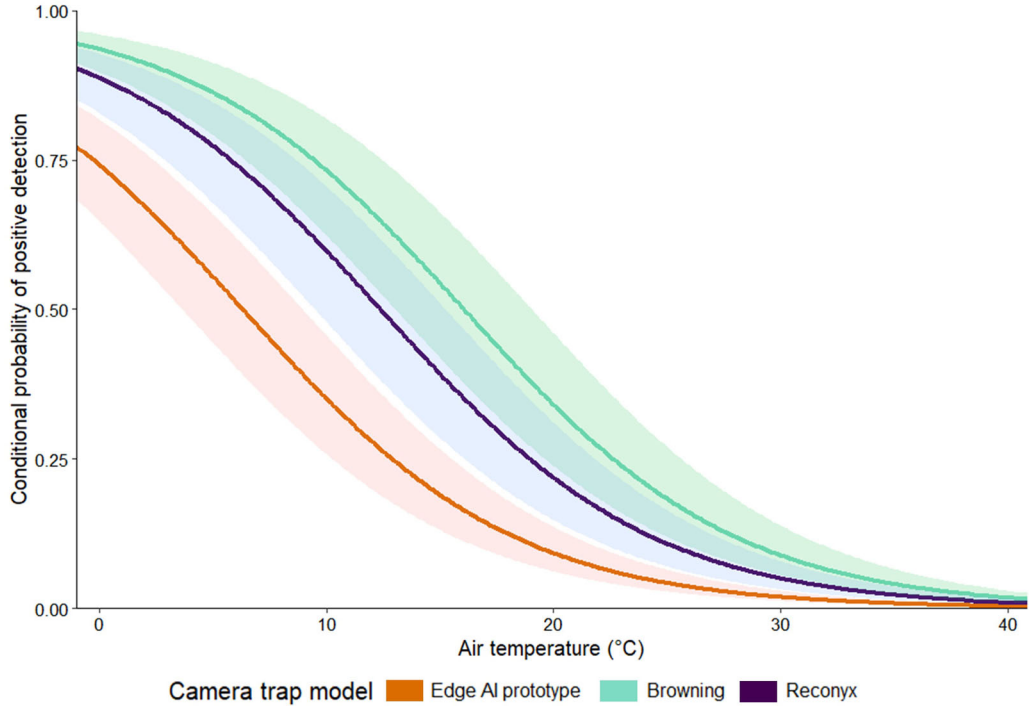

FIGURE 2 Influence of air temperature on the predicted conditional probability of positive detections among 3 camera trap models during summer 2023 in south-central Montana, USA. Shaded areas represent 85% confidence intervals.

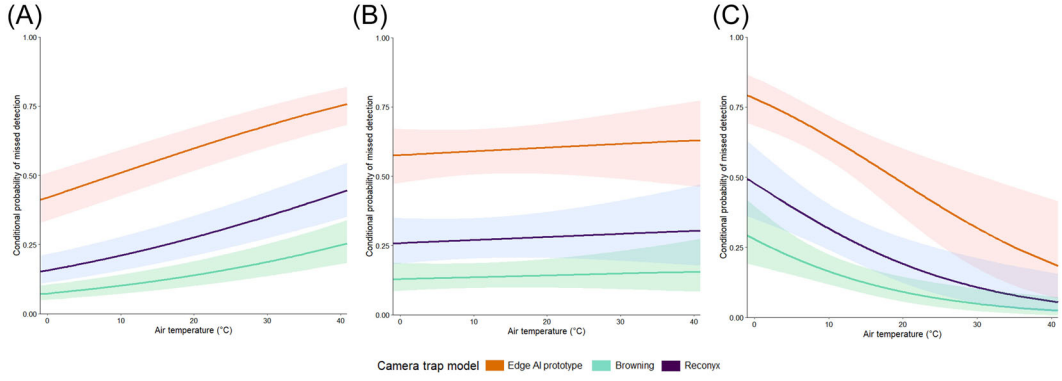

FIGURE 3 Influence of air temperature on the predicted conditional probability of missed detections among 3 camera trap models during summer 2023 in south-central Montana, USA. Responses by the 3 camera trap models are shown relative to air temperature during daytime (A), crepuscular periods (B), and nighttime (C). Shaded areas represent 85% confidence intervals.

from background surface objects (Havens and Sharp 2015). The resulting nighttime thermal contrasts between animal and background object surfaces are greater when air temperatures are high, making missed detections less likely. However, the temperature differential fades during daylight hours when solar radiation causes background surface objects to emit more radiation, making missed detections more probable during

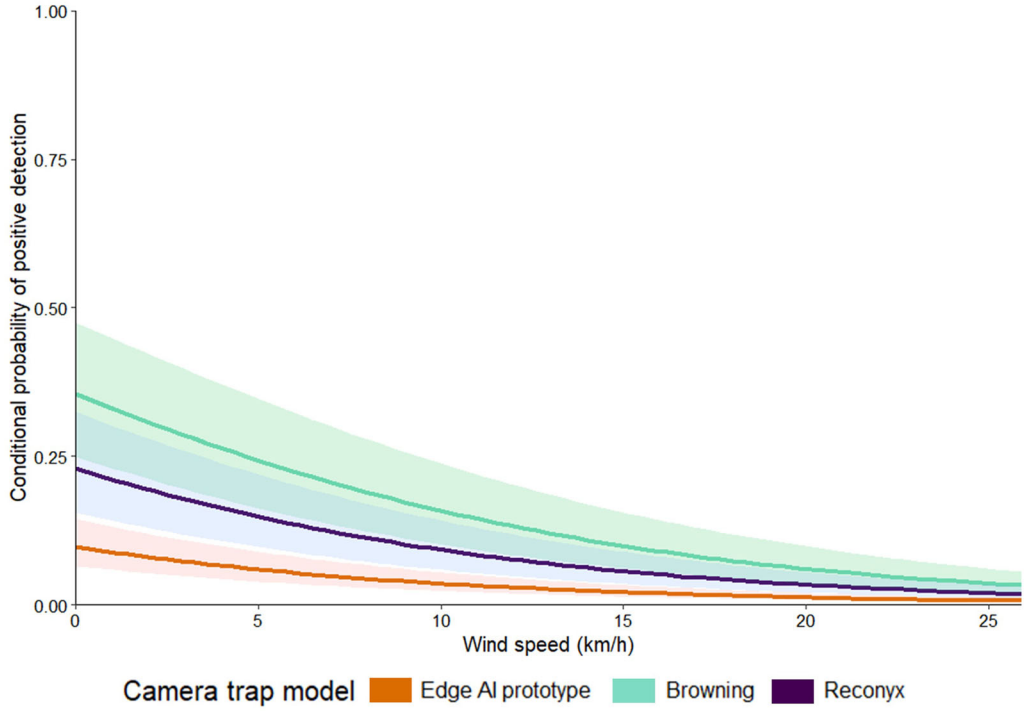

FIGURE 4 Influence of wind speed on the predicted conditional probability of positive detections among 3 camera trap models during summer 2023 in south-central Montana, USA. Shaded areas represent 85% confidence intervals.

daytime when air temperatures are high. Similarly, thermal fluctuations in the environment also led to a higher likelihood of false positives and a lower likelihood of positive detections as air temperature increased.

By principle, the PIR sensor function assumes a homogenous background surface with relatively even amounts of infrared radiation emitted within the detection zone when animals are absent. However, background surfaces such as vegetation, rocks, and bare ground do not emit equivalent amounts of infrared radiation, nor heat or cool at the same rates. Background surface heterogeneity makes PIR sensors susceptible to false positive triggers (Welbourne et al. 2016), and false positive captures can be excessive (Heiniger and Gillespie 2018). The edge AI-enabled prototype in our study effectively filtered out non-animal thermal anomalies by analyzing thermal anomalies before triggering to capture images, and it nearly eliminated the likelihood of capturing false positives regardless of air temperature. However, the advantage of nearly eliminating false positives came at the cost of an increased probability of missed detections, likely due to the stringent filtering mechanisms employed by the AI algorithm, which excluded some legitimate detections. The trade-off underscores the need for further refinement of AI algorithms to balance the reduction of false positives with the risk of missed detections.

Animal behavioral adjustments to warmer air temperatures also made animals more difficult to detect during daytime. The conditional probability of capturing an animal's image decreased when animals were lying down or resting compared to when animals were more active and visible. Elk, mule deer, white-tailed deer, wolves, and grizzly bears are wildlife species documented to reduce activity when air temperatures approach the upper critical threshold of their thermal neutral zone (Parker and Robbins 1984, Harting 1985, Beier and McCullough 1990, Bryce et al. 2022). For example, mule deer and grizzly bears reduce their activity when summer air temperatures exceed 20°C (Parker and Robbins 1984, Harting 1985). Horses and cattle rest more when summer air temperatures exceed 25°C and 29°C, respectively (Dwyer 1961, Snoeks et al. 2015). Animals also respond to warmer air temperatures during summer by

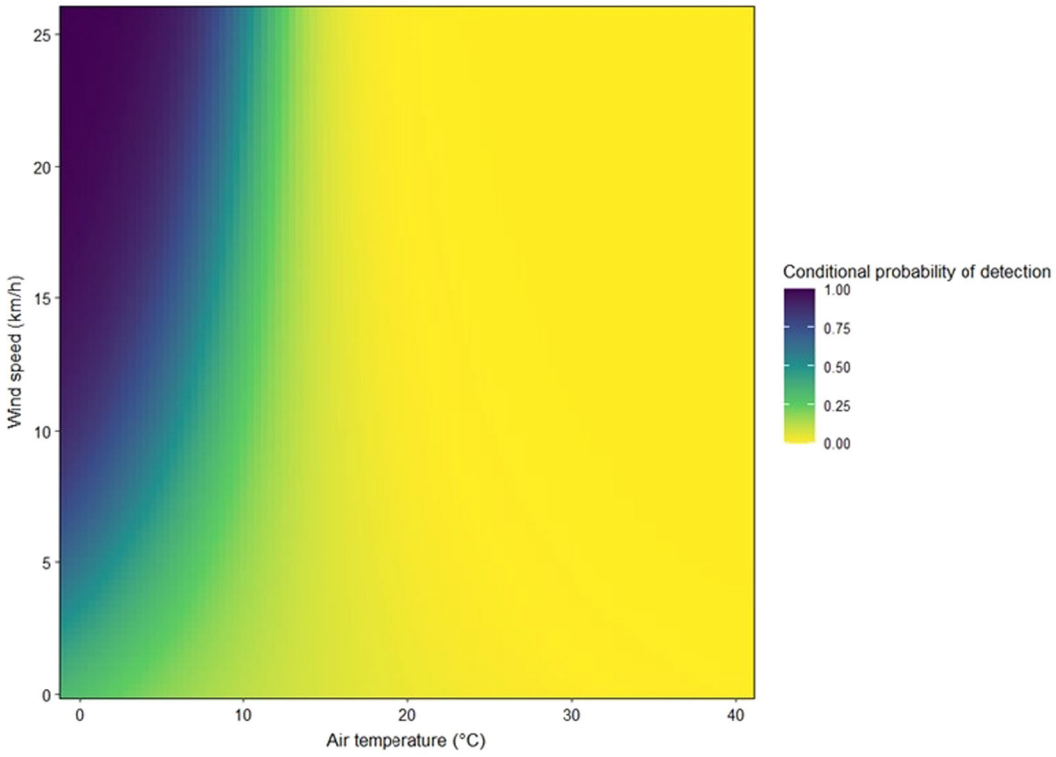

FIGURE 5 Heat map showing the interactive influence of wind speed and air temperature on the predicted conditional probability of positive detections, regardless of camera trap model, during summer 2023 in south-central Montana, USA.

spending more time bedded down to increase conductive heat loss to the ground (Jacobsen 1980, Merrill 1991), making them more challenging to detect. In our study, the conditional probability of positive detections was very low when the air temperature was ≥30°C. Warmer air temperatures also may hinder camera trap performance if a camera trap becomes too hot from being in the sun. When a camera trap's PIR sensor is hotter than the animal and background surfaces, it will not trigger until its PIR sensor cools down, possibly hours later (Apps and Hutt 2018). Several camera trap groups in our study were not shaded from the sun.

Increased wind speed in our study decreased the conditional probability of positive detections by all 3 camera trap models, and the edge AI-enabled camera trap did not mitigate this environmental effect. The effect of wind observed in our study was consistent with the thermodynamic principles that govern heat transfer. When the air temperature was cooler than the background object surface temperatures or animal surface temperatures, heat was transferred from these surfaces to the air and carried away by the wind via forced convection. Increased wind speeds accelerate convective heat loss from animal body surfaces (Moen and Jacobsen 1974, Parker and Gillingham 1990, Merrill 1991), which reduces an animal's thermal signature and makes them more difficult to detect.

Animal behavior also helps explain why conditional detection probabilities decreased as wind speed increased. Prey animals, for example, are more difficult to detect in windy conditions because prey animals reduce their activity when wind noise and moving vegetation impede auditory and olfactory cues that can make prey more vulnerable to predation (Cherry and Barton 2017, Studd et al. 2022). Grizzly bear activity is generally unaffected by increased wind speeds during summer (Harting 1985), while another large predator, Canada lynx (*Lynx canadensis*), is more active on windy days (Studd et al. 2022). Olfactory mesopredators, including red fox, striped skunk (*Mephitis mephitis*), and raccoon (*Procyon lotor*), reduced activity at wind speeds >7 to 14 km/h in northern Utah, USA (Ruzicka and Conover 2011).

Cloud cover did not significantly affect camera trap performance in our study. We expected that water droplets or ice crystals in clouds would attenuate the amount of solar radiation that reached the Earth's surface, thereby limiting background surface temperatures and increasing conditional detection probabilities due to enhanced thermal signature contrasts between animals and landscape features (Havens and Sharp 2015). For example, overcast skies enhance positive detections in aerial wildlife surveys using forward-looking infrared imagery (FLIR; Bernatas and Nelson 2004), but in our study, cloud cover did not affect the conditional probability of positive detections, false positives, or missed detections, regardless of the camera trap model. However, our cloud cover data did not differentiate among different types of cloud cover (e.g., low, thick clouds vs. high, thin clouds vs. partly cloudy skies). More discriminating measures of cloud cover might reveal a more prominent effect on camera trap performance.

We anticipated that camera trap performance would be negatively affected more in our forest vs. grassland sites due to the greater structural heterogeneity of the forest vegetation, but this did not occur. Our results differ from previous research, which documented that uneven heating of sun-warmed tree leaves in a camera trap's detection zone increased the capture of false positive images (Gregory et al. 2014). Our results suggest that the differences in vegetative structure between the forest and grassland vegetation types in our study were insufficient to create a detectable effect on camera trap performance.

MANAGEMENT IMPLICATIONS

Camera trap performance is imperfect. Our results confirm that summer air temperatures, wind speeds, and time of day can affect the performance of camera traps commonly used by contemporary wildlife researchers and managers. We recommend incorporating these environmental variables into estimates of detection probability during summer. We also documented that environmental effects on camera trap performance vary among camera trap models, and we support recommendations that the camera trap model be accounted for (e.g., included as a fixed or random effect) when wildlife surveys involve data collected from 2 or more camera trap models. Finally, the edge AI-enabled camera trap prototype successfully mitigated the effects of warmer air temperatures on false positive captures. However, the edge AI-enabled prototype was also more likely to miss detections than commercially available camera traps without AI. As AI technology advances, the next challenge lies in refining edge AI-enabled camera traps to maintain their advantage in reducing false positives when air temperatures are warm while minimizing missed detections.

ACKNOWLEDGMENTS

The authors thank the landowners and managers of AMB West Ranch, Anderson Ranch, and Reedfly Farm for access to study sites, and C. Goldhahn, Montana State University Statistical Consulting and Research Services, P. Nugent, E. Vincent, A. Kaltenbach, K. Ogg, A. Trauner, and M. Moosbrugger for assistance with data collection and analysis. We thank Editor-in-Chief Collier, Associate Editor Byrne, and 2 anonymous reviewers for their helpful comments and suggestions that improved our manuscript. The Bair Ranch Foundation and Montana Agricultural Experiment Station provided funding.

CONFLICT OF INTEREST STATEMENT

The authors declare no conflicts of interest.

ETHICS STATEMENT

Our data collection was non-invasive and observational. We did not use lures or attractants. or disturb or negatively affect individual animals or populations. We followed the American Society of Mammalogists' guidelines for conducting wildlife research (Sikes and Animal Care and Use Committee of the American Society of Mammalogists 2016).

DATA AVAILABILITY STATEMENT

The data that support the findings of this study are available from the corresponding author upon reasonable request.

ORCID

Taylor L. Kaltenbach https://orcid.org/0009-0003-1761-624X
Lance B. McNew https://orcid.org/0000-0003-0006-7304
Jared T. Beaver https://orcid.org/0000-0002-2285-9356

REFERENCES

Apps, P. J., and J. W. Hutt. 2018. How camera traps work and how to work them. African Journal of Ecology 56:702–709.
Arnold, T. W. 2010. Uninformative parameters and model selection using Akaike's Information Criterion. Journal of Wildlife Management 74:1175–1178.
Beier, P., and D. R. McCullough. 1990. Factors influencing white-tailed deer activity patterns and habitat use. Wildlife Monographs 109:3–51.
Bernatas, S., and L. Nelson. 2004. Sightability model for Californa bighorn sheep in canyonlands using forward-looking infrared (FLIR). Wildlife Society Bulletin 32:638–647.
Bryce, C. M., C. E. Dunford, A. M. Pagano, Y. Wang, B. L. Borg, S. M. Arthur, and T. M. Williams. 2022. Environmental correlates of activity and energetics in a wide-ranging social carnivore. Animal Biotelemetry 10, no. 1: 1–16. https://doi.org/10.1186/s40317-021-00272-w
Burnham, K. P., and D. R. Anderson. 2002. Model selection and multimodel inference: A practical information-theoretic approach. Springer, New York, New York, USA.
Burton, A. C., E. Neilson, D. Moreira, A. Ladle, R. Steenweg, J. T. Fisher, E. Bayne, and S. Boutin. 2015. Wildlife camera trapping: A review and recommendations for linking surveys to ecological processes. Journal of Applied Ecology 52:675–685.
Cherry, M. J., and B. T. Barton. 2017. Effects of wind on predator-prey interactions. Food Webs 13:92–97.
Cilulko, J., P. Janiszewski, M. Bogdaszewski, and E. Szczygielska. 2013. Infrared thermal imaging in studies of wild animals. European Journal of Wildlife Research 59:17–23.
Cutler, T. L., and D. E. Swann. 1999. Using remote photography in wildlife ecology: A review. Wildlife Society Bulletin 27:571–581.
Damm, P. E., J. B. Grand, and S. W. Barnett. 2010. Variation in detection among passive infrared triggered-cameras used in wildlife research. Proceedings of the Annual Conference of the Southeastern Association of Fish and Wildlife Agencies 64:125–130.
Dertien, J. S., H. Negi, E. Dinerstein, R. Krishnamurthy, H. S. Negi, R. Gopal, S. Gulick, S. K. Pathak, M. Kapoor, and P. Yadav. 2023. Mitigating human-wildlife conflict and monitoring endangered tigers using a real-time camera-based alert system. BioScience 73:748–757.
Dwyer, D. D. 1961. Activities and grazing preferences of cows with calves in northern Osage County. Stillwater, OK, USA: Oklahoma Agricultural Experiment Station Bulletin B-588.
Glover-Kapfer, P., C. A. Soto-Navarro, and O. R. Wearn. 2019. Camera trapping version 3.0: Current constraints and future priorities for development. Remote Sensing in Ecology and Conservation 5:209–223.
Green, R. 1979. Equations and test statistic parameters. Pages 109–110 *in* R. Green, editor. Sampling design and statistical methods for environmental biologists. John Wiley and Sons, New York, New York, USA.
Greenberg, S., T. Godin, and J. Whittington. 2019. Design patterns for wildlife-related camera trap image analysis. Ecology and Evolution 9:13706–13730.
Gregory, T., F. Carrasco Rueda, J. Deichmann, J. Kolowski, and A. Alonso. 2014. Arboreal camera trapping: Taking a proven method to new heights. Methods in Ecology and Evolution 5:443–451.
Harting, Jr., A. L. 1985. Relationships between activity patterns and foraging strategies of Yellowstone grizzly bears. Thesis, Montana State University, Bozeman, MT, USA.
Havens, K. J., and E. J. Sharp. 2015. Using thermal imagers for animal ecology. Pages 245–314 *in* K. J. Havens, and E. J. Sharp, editors. Thermal imaging techniques to survey and monitor animals in the wild. Academic Press, Amsterdam, Netherlands.
Heidinger, A. K., M. J. Pavlonis, C. Calvert, J. Hoffman, S. Nebuda, W. Straka, III, A. Walther, and S. Wanzong. 2020. ABI cloud products from the GOES-R Series. Pages 43–62 *in* S. J. Goodman, T. J. Schmit, J. Daniels, and R. J. Redmon, editors. The GOER-R Series: A new generation of geostationary environmental satellites. Elsevier, Cambridge, Massachusetts, USA.

Heidinger, A., and W. C. Straka, III. 2012. ABI cloud mask, version 3.0. National Environmental Satellite, Data, and Information Service, Center for Satellite Applications and Research, National Oceanic and Atmospheric Administration.

Heiniger, J., and G. Gillespie. 2018. High variation in camera trap-model sensitivity for surveying mammal species in northern Australia. Wildlife Research 45:578–585.

Hofmeester, T. R., J. P. Cromsigt, J. Odden, H. Andrén, J. Kindberg, and J. D. Linnell. 2019. Framing pictures: A conceptual framework to identify and correct for biases in detection probability of camera traps enabling multi-species comparison. Ecology and Evolution 9:2320–2336.

Hosmer, D. W., and S. Lemeshow. 2000. Applied logistic regression. Second edition. Wiley, New York, New York, USA.

Hughson, D. L., N. W. Darby, and J. D. Dungan. 2010. Comparison of motion-activated cameras for wildlife investigations. California Fish and Game 96:101–109.

Iannarilli, F., J. Erb, T. W. Arnold, and J. R. Fieberg. 2021. Evaluating species-specific responses to camera-trap survey designs. Wildlife Biology 2021:1–12.

Jacobs, C. E., and D. E. Ausband. 2018. An evaluation of camera trap performance–What are we missing and does deployment height matter? Remote Sensing in Ecology and Conservation 4:352–360.

Jacobsen, N. K., 1980. Differences of thermal properties of white-tailed deer pelage between seasons and body regions. Journal of Thermal Biology 5:151–158.

Jessop, T. S., B. Holmes, A. Sendjojo, M. O. Thorpe, and E. G. Ritchie. 2021. Assessing the benefits of integrated introduced predator management for recovery of native predators. Restoration Ecology 29:e13419.

Kays, R., B. Kranstauber, P. Jansen, C. Carbone, M. Rowcliffe, T. Fountain, and S. Tilak. 2009. Camera traps as sensor networks for monitoring animal communities. Pages 811–818 *in* Proceedings of the Institute of Electrical and Electronics Engineers 34th Conference on Local Computer Networks.

Lüdecke, D. 2018. ggeffects: Tidy data frames of marginal effects from regression models. Journal of Open Source Software 3:772.

Meek, P. D., A. G. Ballard, and P. J. S. Fleming. 2012. An introduction to camera trapping for wildlife surveys in Australia. Canberra, Australia: Invasive Animals Cooperative Research Centre.

Meek, P. D., G. A. Ballard, and P. S. Fleming. 2015. The pitfalls of wildlife camera trapping as a survey tool in Australia. Australian Mammalogy 37:13-22.

Meek, P. D., and A. Pittet. 2012. User-based design specifications for the ultimate camera trap for wildlife research. Wildlife Research 39:649-660.

Merrill, E. H. 1991. Thermal constraints on use of cover types and activity time of elk. Applied Animal Behaviour Science 29: 251–267.

Moen, A. N., and F. L. Jacobsen. 1974. Changes in radiant temperature of animal surfaces with wind and radiation. Journal of Wildlife Management 38:366–368.

Montanholi, Y. R., N. E. Odongo, K. C. Swanson, F. S. Schenkel, B. W. McBride, and A. P. Miller. 2008. Application of infrared thermography as an indicator of heat and methane production and its use in the study of skin temperature in response to physiological events in dairy cattle (*Bos taurus*). Journal of Thermal Biology 33:468-475.

Monterroso, P., F. Rocha, S. van Wyk, T. António, M. Chicomo, S. Kosmas, F. Lages, E. Fabiano, and R. Godinho. 2020. Updated ranges of the Vulnerable cheetah and Endangered African wild dog in Angola. Oryx 54:851–853.

Mosley, J. C., J. Fidel, H. E. Hunter, P. O. Husby, C. E. Kay, J. G. Mundinger, and R. M. Yonk. 2018. An ecological assessment of the Northern Yellowstone Range: Introduction to the special issue. Rangelands 40:173–176.

Mosley, J. C., and J. G. Mundinger. 2018. History and status of wild ungulate populations on the Northern Yellowstone Range. Rangelands 40:189–201.

Mosley, J. C., B. L. Roeder, R. A. Frost, S. L. Wells, L. B. McNew, and P. E. Clark. 2020. Mitigating human conflicts with livestock guardian dogs in extensive sheep grazing systems. Rangeland Ecology and Management 73:724–732.

Mota-Rojas, D., A. Ogi, D. Villanueva-Garcia, I. Hernandez-Avalos, A. Casas-Alvarado, A. Dominguez-Oliva, P. Lendez, and M. Ghezzi. 2024. Thermal imaging as a method to indirectly assess peripheral vascular integrity and tissue viability in veterinary medicine: Animal models and clinical applications. Animals 14: Article 142.

Mueggler, W., and W. Stewart. 1980. Grassland and shrubland habitat types of western Montana. US Department of Agriculture, Forest Service, Intermountain Forest and Range Experiment Station, General Technical Report INT-66, Ogden, UT, USA.

Newey, S., P. Davidson, S. Nazir, G. Fairhurst, F. Verdicchio, R. J. Irvine, and R. van der Wal. 2015. Limitations of recreational camera traps for wildlife management and conservation research: A practitioner's perspective. Ambio 44:624–635.

Palencia, P., R. Vada, S. Zanet, M. Calvini, A. De Giovanni, G. Gola, and E. Ferroglio. 2023. Not just pictures: Utility of camera trapping in the context of African swine fever and wild boar management. Transboundary and Emerging Diseases 2023:1–9.

Parker, K. L., and M. P. Gillingham. 1990. Estimates of critical thermal environments for mule deer. Journal of Range Management 43:73–81.

Parker, K. L., and C. T. Robbins. 1984. Thermoregulation in mule deer and elk. Canadian Journal of Zoology 62:1409–1422.
Pfister, R. D., B. L. Kovalchik, S. F. Arno, and R. C. Presby. 1977. Forest habitat types of Montana. US Department of Agriculture, Forest Service, Intermountain Forest and Range Experiment Station, General Technical Report INT-34, Ogden, UT, USA.
Rockhill, A. P., C. S. DePerno, and R. A. Powell. 2013. The effect of illumination and time of day on movements of bobcats (*Lynx rufus*). PLoS ONE 8:e69213.
Rovero, F., and F. Zimmermann. 2016. Camera features related to specific ecological applications. Pages 8–21 *in* F. Rovero, and F. Zimmermann, editors. Camera Trapping for Wildlife Research. Pelagic Publishing Exeter, Exeter, UK.
Rowcliffe, M. J., C. Carbone, P. A. Jansen, R. Kays, and B. Kranstauber. 2011. Quantifying the sensitivity of camera traps: An adapted distance sampling approach. Methods in Ecology and Evolution 2:464–476.
Ruzicka, R. E., and M. R. Conover. 2011. Influence of wind and humidity on foraging behavior of olfactory mesopredators. Canadian Field-Naturalist 125:132–139.
Schielzeth, H. 2010. Simple means to improve the interpretability of regression coefficients. Methods in Ecology and Evolution 1:103–113.
Sikes, R. S., and Animal Care and Use Committee of the American Society of Mammalogists. 2016. 2016 Guidelines of the American Society of Mammalogists for the use of wild mammals in research and education. Journal of Mammalogy 97: 663–688.
Snoeks, M. G., C. P. H. Moons, F. O. Odberg, M. Aviron, and R. Geers. 2015. Behavior of horses on pasture in relation to weather and shelter–A field study in a temperate climate. Journal of Veterinary Behavior 10:561–568.
Studd, E. K., M. J. L. Peers, A. K. Menzies, R. Derbyshire, Y. N. Majchrzak, J. L. Seguin, D. L. Murray, B. Dantzer, J. E. Lane, A. G. McAdam, et al. 2022. Behavioural adjustments of predators and prey to wind speed in the boreal forest. Oecologia 200:349–358.
Swann, D. E., C. C. Hass, D. C. Dalton, and S. A. Wolf. 2004. Infrared-triggered cameras for detecting wildlife: An evaluation and review. Wildlife Society Bulletin 32:357–365.
Swanson, A., M. Kosmala, C. Lintott, R. Simpson, A. Smith, and C. Packer. 2015. Snapshot Serengeti, high-frequency annotated camera trap images of 40 mammalian species in an African savanna. Scientific Data 2:1–14.
Welbourne, D. J., A. W. Claridge, D. J. Paull, and A. Lambert. 2016. How do passive infrared triggered camera traps operate and why does it matter? Breaking down common misconceptions. Remote Sensing in Ecology and Conservation 2: 77–83.
Wellington, K., C. Bottom, C. Merrill, and J. A. Litvaitis. 2014. Identifying performance differences among trail cameras used to monitor forest mammals. Wildlife Society Bulletin 38:634–638.
Whytock, R. C., T. Suijten, T. van Deursen, J. Świezewski, H. Mermiaghe, N. Madamba, N. Mouckoumou, J. A. Zwerts, A. F. K. Pambo, and L. Bahaa-el-din. 2023. Real-time alerts from AI-enabled camera traps using the Iridium satellite network: A case-study in Gabon, central Africa. Methods in Ecology and Evolution 10:80–91.
Zimmermann, F., and F. Rovero. 2016. Field deployment of camera traps. Pages 22–32 *in* F. Rovero, and F. Zimmermann, editors. Camera Trapping for Wildlife Research. Pelagic Publishing, Exeter, UK.

Associate Editor: Michael Byrne.

How to cite this article: Kaltenbach, T. L., J. C. Mosley, L. B. McNew, and J. T. Beaver. 2025. Can edge AI mitigate environmental effects on camera trap performance? Wildlife Society Bulletin 49:e1598. https://doi.org/10.1002/wsb.1598